Alkali Metals

DOI: 10.1002/anie.201207962

Potassium–Alkane Interactions within a Rigid Hydrophobic Pocket**

*Nicholas R. Andreychuk and David J. H. Emslie**

Metal–alkane complexes are of importance because of their involvement in alkane C–H activation reactions[1] and hydrocarbon adsorption in alkali-metal-containing zeolites.[2] However, observable metal–alkane complexes are scarce as a consequence of the poor donor/acceptor character of alkanes and the low polarity of C–H bonds. Examples detected by NMR spectroscopy include $[(C_5R_5)Re(CO)_2(alkane)]$,[3,4] $[(C_5R_5)M(CO)(PF_3)(alkane)]$ (M = Re or Mn),[4] $[TpRe(CO)_2(alkane)]$,[5] $[(PONOP)Rh(CH_4)]^+$ {PONOP = 2,6-($tBu_2PO)_2C_5H_3N$},[6] and $[(C_6Et_6)W(CO)_2(n\text{-pentane})]$,[7] but none of these complexes have proven sufficiently robust to allow isolation or crystallization. At the other end of the spectrum are the crystallographically characterized metal–alkane complexes[8] which have not been observed in solution. The only members of this group are the iron(II) double A-frame porphyrin–heptane complex reported by Reed and co-workers,[9] the uranium(III)–alkane complexes reported by Meyer and co-workers,[10] and a rhodium(I) norbornane complex reported by Weller and co-workers,[11] and in all cases the metal–alkane interaction is considered to possess some degree of covalency, perhaps with additional stabilization from interactions between the alkane and the ligand framework. Herein we describe potassium complexes of a new highly rigid and sterically encumbered NON-donor ligand, all of which feature remarkably short intermolecular potassium–alkane distances in the solid state.

Palladium-catalyzed coupling of 4,5-dibromo-2,7-di-*tert*-butyl-9,9-dimethylxanthene with 2 equivalents of 2,6-dimesitylaniline afforded 4,5-bis(2,6-dimesitylanilino)-2,7-di-*tert*-butyl-9,9-dimethylxanthene [H_2(XAT); Scheme 1], which is an extremely sterically hindered analogue of the known 4,5-bis(2,6-diisopropylanilino)-2,7-di-*tert*-butyl-9,9-dimethylxanthene[12] and 4,5-bis(2,4,6-trimethylanilino)-2,7-di-*tert*-butyl-9,9-dimethylxanthene[13] pro-ligands. Reaction of H_2(XAT) with excess KH in toluene yielded the dipotassium salt, and filtration and layering with hexanes at −30 °C deposited vibrant yellow X-ray quality crystals of $[K_2(XAT)(n\text{-hexane})]\cdot$toluene (**1**; Scheme 1 and Figure 1). The potassium atoms in **1** are bound to bridging amido and ether donors, forming

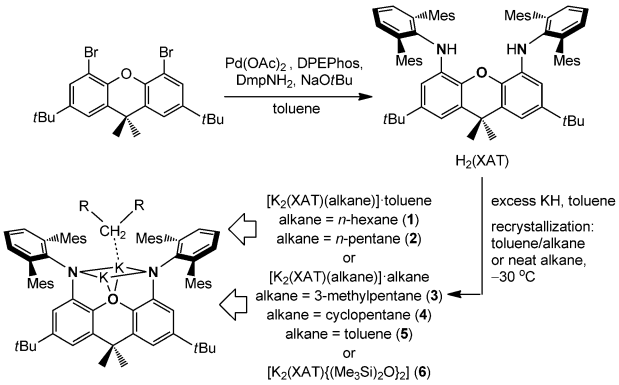

Scheme 1. Synthesis of H_2(XAT) and **1**–**6**. DPEPhos = bis{2-(diphenylphosphino)phenyl}ether], Dmp = 2,6-dimesitylphenyl, Mes = mesityl.

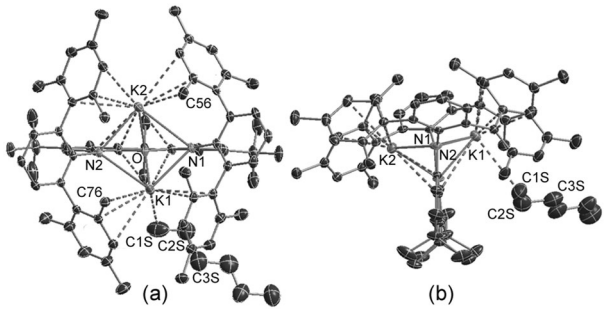

Figure 1. Two views of the X-ray crystal structure of $[K_2(XAT)(n\text{-hexane})]\cdot$toluene (**1**). Hydrogen atoms and lattice solvent are omitted for clarity and ellipsoids are at 50% probability. K-C distances less than 3.50 Å are highlighted as dotted lines.

a square pyramidal K_2N_2O core with oxygen in the apical site. However, an unexpected feature is the close approach of a molecule of *n*-hexane to K(1), with a K(1)-C(1S) distance of 3.284(4) Å.

The Fe-C distances in Reed's iron porphyrin heptane complex are 2.5 and 2.8 Å (the heptane molecule and the Fe atoms are disordered; calculated Fe-C distances for methane, ethane, propane, and butane complexes are 2.68–2.70 Å),[9] the U-C distances in Meyer's uranium–alkane complexes range from 3.731(8) to 3.864(7) Å (the calculated U-C distance for the methylcyclohexane complex is 3.974 Å),[10] and the Rh-C distances in Weller's rhodium norbornane complex are 2.480(11) and 2.494(10) Å.[11] To enable a rough comparison between the M-C (M = metal) distances in the more ionic uranium complex and complex **1**, ionic radii for U^{3+} and K^+ (1.03 and 1.38 Å for a coordination number of six)[14] may be subtracted from the crystallographic M-C distances, yielding values of 2.70–2.83 and 1.90 Å, respectively. The K-C distance in complex **1** is therefore notably

[*] N. R. Andreychuk, Prof. D. J. H. Emslie
Department of Chemistry, McMaster University
1280 Main Street West, Hamilton, ON, L8S 4M1 (Canada)
E-mail: emslied@mcmaster.ca
Homepage: http://www.chemistry.mcmaster.ca/emslie/emslie.html

[**] D.J.H.E. thanks the NSERC of Canada for a Discovery Grant. N.R.A. thanks the NSERC of Canada and the province of Ontario for CGS-M and OGS support. We are also grateful to H. A. Jenkins for help with X-ray crystallography, and to P. W. Ayers and I. Vargas-Baca for helpful discussions regarding DFT calculations.

Supporting information for this article is available on the WWW under http://dx.doi.org/10.1002/anie.201207962.

© 2013 Wiley-VCH Verlag GmbH & Co. KGaA, Weinheim

short, and even falls at the lower end of the range of K-C distances observed for face-on potassium–benzene and potassium–toluene interactions, which are typically 3.2 to 3.5 Å.[15,16] The potassium–alkane interaction in **1** can be surmised to involve a weak electrostatic (primarily cation-induced dipole)[17] potassium–alkane interaction stabilized by interactions between the alkane and the hydrophobic ligand pocket.

An analogous intermolecular potassium–alkane interaction is not observed at K(2), perhaps as a result of crystal packing forces as the *para*-methyl carbon C(48) of a mesityl group in an adjacent [K_2(XAT)(*n*-hexane)] molecule is positioned 3.538(3) Å from K(2). However, both potassium atoms in **1** are forced into close proximity with flanking mesityl groups and the xanthene backbone, leading to a large number of K-C_{arene} and K-C_{methyl} distances that are below 3.50 Å (Figure 1). In particular, the intramolecular K-C_{methyl} distances K(2)-C(56) and K(1)-C(76) are 3.180(3) and 3.230(3) Å, respectively. For comparison, the intramolecular K–CHR_3 interactions in the sterically encumbered [{KSi($SiMe_3$)$_3$}$_2$],[16] [$KC(SiMe_3)_3]_n$,[18] and [K_2(O{$SiMe_2$C($SiHMe_2$)$_2$}]$_n$[19] range from 3.138(3) to 3.433(3) Å.

To further probe the disposition of the K_2(XAT) moiety to interact with the hydrocarbon solvent, alternative crystallization conditions were explored, yielding X-ray quality crystals of [K_2(XAT)(*n*-pentane)]·toluene (**2**), [K_2(XAT)(3-methylpentane)]·3-methylpentane (**3**), [K_2(XAT)(cyclopentane)]·cyclopentane (**4**), [K_2(XAT)(toluene)]·0.5toluene (**5**), and [K_2(XAT){$(Me_3Si)_2O$}$_2$] (**6**) (Scheme 1 and Figure 2). The central core of structures **2**–**6** is analogous to that in **1** (each potassium atom is NON-coordinated and engages in intramolecular potassium–carbon interactions with surrounding mesityl groups), and in every case either one (**2**–**5**) or two (**6**) intermolecular K–H_3CR or K–H_2CR_2 interactions are observed. These interactions involve the 1-position of *n*-pentane and 3-methylpentane, one of the CH_2 groups in cyclopentane, and a methyl group of toluene and hexamethyldisiloxane, leading to K-C distances of 3.358(5) Å in **2**, 3.215(5) Å in **3**, 3.48(1) and 3.62(3) Å in **4**,[20] 3.285(7) and 3.305(9) Å in **5**, and 3.282(5) and 3.332(5) Å in **6** (bound cyclopentane in **4** and toluene in **5** are disordered over 2 positions). In **5**, toluene bridges between adjacent molecules through K–C_{arene} interactions with distances of 3.240(7), 3.425(9), and 3.433(8) Å (Figure 2). The K-C-C angles in primary alkyl complexes **1**, **2**, and **3** are 117°, 154°, and 170°, respectively, the K-C_{methyl}-C angles in **5** are 99° and 108°, and the K-C-Si angles in **6** are 171 and 176°.

Compounds **1**–**6** illustrate the extent to which intermolecular K–H_3CR and K–H_2CR_2 interactions are a common feature of the solid-state structures of K_2(XAT). However, attempts to observe alkane or O($SiMe_3$)$_2$ binding by ^{1}H or ^{13}C NMR spectroscopy in 3-methylpentane/[D_8]toluene (−80 °C), 3-methylpentane (−110 °C), cyclopentane (−80 °C), or O($SiMe_3$)$_2$ (−60 °C; ^{1}H NMR spectroscopy only) were unsuccessful, possibly as a result of rapid exchange between free and bound solvent.

DFT calculations (ADF 2012.01, BLYP with and without Grimme's DFT-D3-BJ dispersion correction, TZ2P all-electron, gas phase, VWN, ZORA) were carried out to probe the nature of the potassium–alkane interaction in **3**, which is the complex with the shortest K-C_{alkane} distance. Geometry optimization using the BLYP-D3-BJ functional yielded a substantially shorter K-C_{alkane} interaction (3.218 Å) than was observed using BLYP (4.176 Å), and is consistent with significant stabilization of the potassium–alkane interaction through dispersion interactions. The calculated K-C_{alkane} distance in **3** shows excellent agreement with the crystallographic distance [3.215(5) Å], and the three hydrogen atoms on C(1S) are located 2.82, 3.08, and 3.15 Å from K(1). The BLYP-D3-BJ functional also adequately reproduced the K-C-C angle (168.1°; see 170.2° in the X-ray crystal structure), the conformation of 3-methylpentane, and the K-N, K-O, and intramolecular K-C distances. However, the exact position of 3-methylpentane (especially the two more remote carbon atoms), within the binding pocket deviates to some extent from that in the X-ray structure (see Figure S4 in the Supporting Information).

Complex **3** was investigated through a fragment approach which considered the interaction between the K_2(XAT) and 3-methylpentane fragments in the geometries adopted in the calculated structure of **3**. Within this approach, the energy decomposition analysis[21] of Ziegler and Rauk[22] (ΔE_{int} =

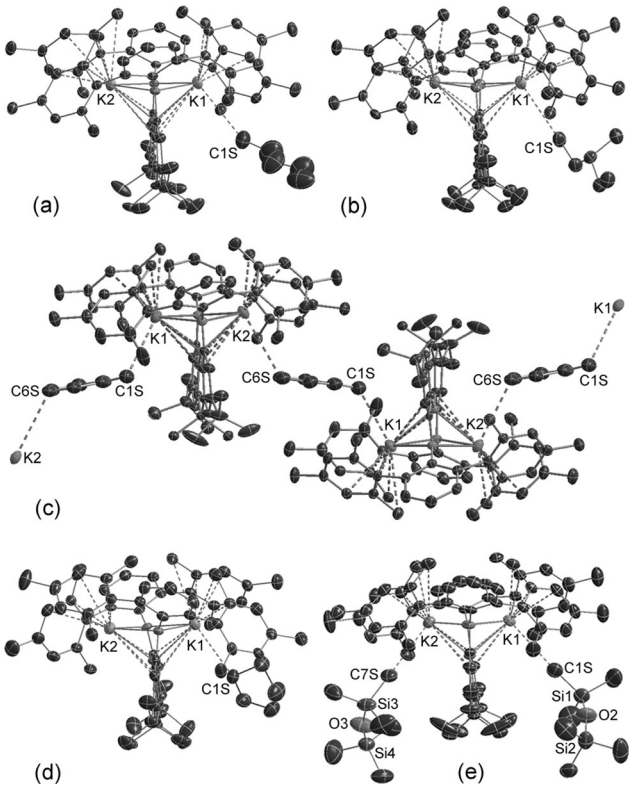

Figure 2. X-ray crystal structures of a) [K_2(XAT)(*n*-pentane)]·toluene (**2**), b) [K_2(XAT)(3-methylpentane)]·3-methylpentane (**3**), c) [K_2(XAT)-(toluene)]·0.5toluene (**5**), d) [K_2(XAT)(cyclopentane)]· cyclopentane (**4**), and e) [K_2(XAT){$(Me_3Si)_2O$}$_2$] (**6**). Hydrogen atoms and lattice solvent are omitted for clarity. Only one of the two orientations of cyclopentane and toluene are shown in the structures of **4** and **5**. Ellipsoids are shown at 50% probility for **2**–**5** (collected at 100 K) and 30% probability for **6** (collected at 223 K). K-C distances below 3.50 Å are highlighted as dotted lines.

 © 2013 Wiley-VCH Verlag GmbH & Co. KGaA, Weinheim

$\Delta E_{elec} + \Delta E_{orb} + \Delta E_{disp} + \Delta E_{Pauli}$; BSSE correction included) yielded a total interaction energy (ΔE_{int}) of $-54.2\ kJ\,mol^{-1}$, which comprises $\Delta E_{elec} = -31.6\ kJ\,mol^{-1}$ (electrostatic interaction energy, calculated using frozen charge distributions for both fragments), $\Delta E_{orb} = -16.6\ kJ\,mol^{-1}$ (orbital interaction energy; this term includes all contributions resulting from intrafragment polarization), $\Delta E_{disp} = -87.3\ kJ\,mol^{-1}$ (dispersion interactions), and $\Delta E_{Pauli} = 81.2\ kJ\,mol^{-1}$ (Pauli repulsion). The total interaction energy, ΔE_{int}, differs from the true interaction energy only by the energy needed to bring the fragments from their optimum geometries to their geometries in **3**. This preparation energy (ΔE_{prep}) is less than 5% of the value of ΔE_{int}.

The closed-shell interactions (ΔE_{disp} and ΔE_{Pauli}) roughly cancel out, leaving a net contribution of $-6.0\ kJ\,mol^{-1}$. ΔE_{int} is therefore approximately equal to $\Delta E_{elec} + \Delta E_{orb}$. The SCF deformation density isosurfaces in Figure 3 highlight both the

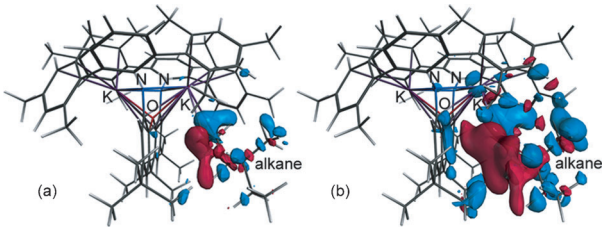

Figure 3. SCF deformation density isosurfaces (set to ± 0.0005 in a and ± 0.0002 in b) from fragment analysis of **3**. Blue represents increased electron density and red represents depleted electron density relative to the initial K_2XAT and 3-methylpentane fragments.

degree of polarization within the alkane fragment and the extent to which the electron density around potassium remains largely unchanged, indicating that ΔE_{orb} is primarily due to a cation-induced dipole electrostatic interaction rather than σ-donation from alkane C–H bonds to potassium. Negligible Hirshfeld charges on the K_2(XAT) and alkane fragments ($< \pm 0.003$) support this interpretation.

Calculations were also performed on a simplified model for **3** (structure **3′**) in which XAT methyl and mesityl groups have been replaced by hydrogen atoms, but the coordinates of all other atoms are identical to those in the BLYP-D3-BJ/TZ2P structure of **3**. This model lacks much of the hydrophobic pocket surrounding the metal, and fragment analysis yielded values of −32.3, −15.8, −10.7, −36.5, and $30.6\ kJ\,mol^{-1}$ for ΔE_{int}, ΔE_{elec}, ΔE_{orb}, ΔE_{disp}, and ΔE_{Pauli}, respectively. The less-negative interaction energy in **3′** highlights the importance of the hydrophobic pocket in stabilizing the potassium–alkane interaction. However, $\Delta E_{disp} - \Delta E_{Pauli}$ is approximately the same in **3** and **3′**, so the more-negative interaction energy for **3** can be considered to arise from more-negative ΔE_{elec} and ΔE_{orb} contributions. Differences in ΔE_{elec} will primarily reflect the number of electron–nucleus interactions between the alkane and the ligand framework, and the more negative ΔE_{orb} for **3** versus **3′** implies stabilization of the polarized alkane through interactions with the surrounding pocket (Figure 3b indicates polarization of the adjacent ligand framework by the polarized alkane). The ability of the hydrophobic binding pocket to stabilize the potassium–alkane interaction in **3** therefore extends beyond the realm of dispersion interactions.

In summary, this work presents the first main-group-metal–alkane interactions to have been observed crystallographically, and provides a unique opportunity for the computational study of well-defined potassium–alkane interactions. The combination of cation-induced dipole electrostatic bonding supported by interactions between the alkane and the surrounding framework is a feature common to both **3** and the potassium–alkane interactions proposed to occur in certain potassium-containing zeolites.[2] The effectiveness of the rigid hydrophobic binding pocket in K_2(XAT) to promote and stabilize even very weak potassium–alkane interactions (as shown crystallographically in the solid state and computationally in the gas phase) also suggests that in combination with catalytically relevant metals, ligands featuring a rigid hydrophobic binding pocket may have untapped potential in alkane C–H activation chemistry.

Experimental Section

Full experimental and characterization details for H_2(XAT) and **1**–**6**, and the details of DFT calculations on structures **3** and **3′** are included in the Supporting Information. CCDC 903943 (**1**), 903944 (**2**), 903945 (**5**), 903946 (**4**), 903947 (**3**) and 903948 (**6**) contain the supplementary crystallographic data for this paper. These data can be obtained free of charge from The Cambridge Crystallographic Data Centre via www.ccdc.cam.ac.uk/data_request/cif.

Received: October 2, 2012
Published online: January 4, 2013

Keywords: alkali metals · alkanes · ligand design · noncovalent interactions · potassium

[1] a) B. A. Arndtsen, R. G. Bergman, T. A. Mobley, T. H. Peterson, *Acc. Chem. Res.* **1995**, *28*, 154–162; b) J. A. Labinger, J. E. Bercaw, *Nature* **2002**, *417*, 507–514; c) R. H. Crabtree, *J. Chem. Soc. Dalton Trans.* **2001**, 2437–2450.

[2] a) A. M. Ferrari, K. M. Neyman, S. Huber, H. Knozinger, N. Rosch, *Langmuir* **1998**, *14*, 5559–5567; b) S. Calero, D. Dubbeldam, R. Krishna, B. Smit, T. J. H. Vlugt, J. F. M. Denayer, J. A. Martens, T. L. M. Maesen, *J. Am. Chem. Soc.* **2004**, *126*, 11377–11386; c) B. Liu, B. Smit, *Phys. Chem. Chem. Phys.* **2006**, *8*, 1852–1857.

[3] a) S. Geftakis, G. E. Ball, *J. Am. Chem. Soc.* **1998**, *120*, 9953–9954; b) J. A. Calladine, O. Torres, M. Anstey, G. E. Ball, R. G. Bergman, J. Curley, S. B. Duckett, M. W. George, A. I. Gilson, D. J. Lawes, R. N. Perutz, X. Z. Sun, K. P. C. Vollhardt, *Chem. Sci.* **2010**, *1*, 622–630.

[4] G. E. Ball, C. M. Brookes, A. J. Cowan, T. A. Darwish, M. W. George, H. K. Kawanami, P. Portius, J. P. Rourke, *Proc. Natl. Acad. Sci. USA* **2007**, *104*, 6927–6932.

[5] S. B. Duckett, M. W. George, O. S. Jina, S. L. Matthews, R. N. Perutz, X. Z. Sun, K. Q. Vuong, *Chem. Commun.* **2009**, 1401–1403.

[6] W. H. Bernskoetter, C. K. Schauer, K. I. Goldberg, M. Brookhart, *Science* **2009**, *326*, 553–556.

[7] R. D. Young, D. J. Lawes, A. F. Hill, G. E. Ball, *J. Am. Chem. Soc.* **2012**, *134*, 8294–8297.

 © 2013 Wiley-VCH Verlag GmbH & Co. KGaA, Weinheim

[8] The binding of ethane and propane to iron centers in an extended metal–organic framework was recently characterized by neutron diffraction: E. D. Bloch, W. L. Queen, R. Krishna, J. M. Zadrozny, C. M. Brown, J. R. Long, *Science* **2012**, *335*, 1606–1610.
[9] D. R. Evans, T. Drovetskaya, R. Bau, C. A. Reed, P. D. W. Boyd, *J. Am. Chem. Soc.* **1997**, *119*, 3633–3634.
[10] I. Castro-Rodriguez, H. Nakai, P. Gantzel, L. N. Zakharov, A. L. Rheingold, K. Meyer, *J. Am. Chem. Soc.* **2003**, *125*, 15734–15735.
[11] S. D. Pike, A. L. Thompson, A. G. Algarra, D. C. Apperley, S. A. Macgregor, A. S. Weller, *Science* **2012**, *337*, 1648–1651.
[12] C. A. Cruz, D. J. H. Emslie, L. E. Harrington, J. F. Britten, C. M. Robertson, *Organometallics* **2007**, *26*, 692–701.
[13] R. M. Porter, A. A. Danopoulos, *Polyhedron* **2006**, *25*, 859–863.
[14] R. D. Shannon, *Acta Crystallogr. Sect. A* **1976**, *32*, 751–767.
[15] a) J. Hao, H. Song, C. Cui, *Organometallics* **2009**, *28*, 3100–3104; b) M. Niemeyer, *Inorg. Chem.* **2006**, *45*, 9085–9095; c) P. B. Hitchcock, M. F. Lappert, R. Sablong, *Dalton Trans.* **2006**, 4146–4154; d) W. J. Evans, D. B. Rego, J. W. Ziller, *Inorg. Chem.* **2006**, *45*, 3437–3443; e) G. C. Forbes, A. R. Kennedy, R. E. Mulvey, B. A. Roberts, R. B. Rowlings, *Organometallics* **2002**, *21*, 5115–5121; f) G. Bai, H. W. Roesky, M. Noltemeyer, H.-G. Schmidt, *J. Chem. Soc. Dalton Trans.* **2002**, 2437–2440; g) C. J. Schaverien, J. B. Vanmechelen, *Organometallics* **1991**, *10*, 1704–1709; h) G. R. Fuentes, P. S. Coan, W. E. Streib, K. G. Caulton, *Polyhedron* **1991**, *10*, 2371–2375.
[16] K. W. Klinkhammer, *Chem. Eur. J.* **1997**, *3*, 1418–1431.
[17] a) E. V. Anslyn, D. A. Dougherty, *Modern physical organic chemistry*, University Science Books, Sausalito, CA, **2006**; b) A. W. Ehlers, C. G. de Koster, R. J. Meier, K. Lammertsma, *J. Phys. Chem. A* **2001**, *105*, 8691–8695.
[18] C. Eaborn, P. B. Hitchcock, K. Izod, A. J. Jaggar, J. D. Smith, *Organometallics* **1994**, *13*, 753–754.
[19] L. J. Bowman, K. Izod, W. Clegg, R. W. Harrington, J. D. Smith, C. Eaborn, *Dalton Trans.* **2006**, 502–508.
[20] The K-C distances in **4** should be viewed with some caution since bound cyclopentane is disordered over two positions and restraints had to be applied to ensure reasonable C–C bond distances (DFIX was used to set all five C-C distances to 1.41 Å with an ESD of 0.01 Å).
[21] F. M. Bickelhaupt, E. J. Baerends in *Reviews in Computational Chemistry*, *Vol. 15* (Eds.: K. B. Lipkowitz, D. B. Boyd), Wiley-VCH, New York, **2000**, pp. 1–86.
[22] a) T. Ziegler, A. Rauk, *Inorg. Chem.* **1979**, *18*, 1755–1759; b) T. Ziegler, A. Rauk, *Inorg. Chem.* **1979**, *18*, 1558–1565.

 © 2013 Wiley-VCH Verlag GmbH & Co. KGaA, Weinheim